JOURNAL OF SOLID STATE CHEMISTRY 34, 263–269 (1980)

The Electronic Structure of $NbSe_3$

ROALD HOFFMANN* AND SASON SHAIK

Department of Chemistry and Materials Science Center, Cornell University, Ithaca, New York 14850

J. C. SCOTT

Department of Physics and Materials Science Center, Cornell University, Ithaca, New York 14850

MYUNG-HWAN WHANGBO* AND MARY J. FOSHEE

Department of Chemistry, North Carolina State University, Raleigh, North Carolina 27650

Received September 24, 1979; in final form December 11, 1979

The electronic structures of monomeric $NbSe_6^{6-}$, dimeric $Nb_2Se_9^{9-}$, and hypothetical and real one-, two-, and three-dimensional structures composed of $NbSe_3$ chains are examined in order to probe the nature of intra- and interchain interactions in this material. The geometrical deformation from perfect trigonal prismatic coordination is crucial, leading to an oxidation state formalism $Nb^{IV}(Sc^{2-})(Se_2^{2-})$. The dimensionality of the conduction bands of $NbSe_3$ is explored.

$NbSe_3$ has furnished a seemingly endless series of electronic surprises (*1*), which is why we have attempted a calculation of the electronic structure of this complex material. Our study takes a chemical viewpoint of the geometrical deformations observed as the full three-dimensional structure is built up. Thus it complements the recently published band structure calculation of Bullett (*2*).

The monoclinic crystals contain as basic building blocks infinite $NbSe_3$ chains parallel to the **b**-axis, emphasized in the schematic diagram of Fig. 1 (*3*). These chains associate in a second dimension along the **c**-axis through Nb–Se interchain contacts that are only slightly longer than those within a chain. The unit cell (Fig. 1) contains six such chains, three of these unrelated by a symmetry operation. The two-dimensional slabs interact weakly in a third dimension along the **a**-axis. The trigonal prismatic coordination and two-dimensional layering of $NbSe_3$ is shared by other transition metal trichalcogenides, but the details of chain interaction and thus the layering pattern differ.

In a very fundamental way we are interested in why any solid-state material assumes the structure that it does. To the chemist a curious feature of the metal trichalcogenide structures is that within the infinite one-dimensional chains a set of three bridging seleniums does not form an equilateral

* To whom correspondence should be addressed.

0022-4596/80/110263-07$02.00/0

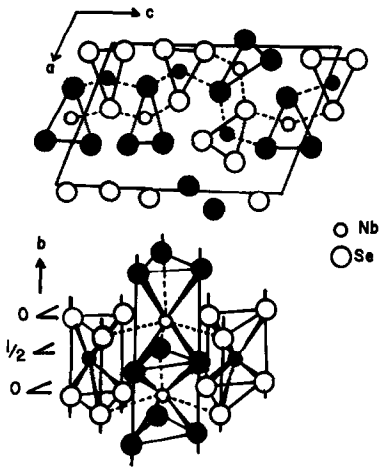

FIG. 1. Schematic representations of the crystal structure of $NbSe_3$.

triangle. Instead one observes a strong asymmetry with Se–Se distances in a typical triangle of 2.37 and 3.81 Å (in one of the chains the distortion is significantly less). The shorter separation is clearly a bonding contact, for instance, only slightly longer than the Se–Se distance in Se_8 (*4a*) or RSe–SeR (*4b*). A similar asymmetry with one Se–Se separation of 2.55 Å has recently been observed in the $W_2Cl_8Se(Se_2)$ dianion (*4c*).

What is the reason for this major distortion? And is it tied to the nature of the conducting electron in this material? Here is what we mean by the last question. If we take the normal oxidation state formalism and apply it to $NbSe_3$ we are led to a formal charge of 6+ for Nb. Given five valence electrons in a Nb atom we are forced to postulate a hole in an inner core Nb level, or much more likely in a band arising from the seleniums. Is this a realistic picture? Another important question concerning $NbSe_3$ is why this material exhibits pseudo-one-dimensional metallic properties along the chain axis (*2*, *3*) despite the seemingly strong interchain Nb–Se interactions along the c-axis as suggested by the crystal structure.

Oxidation State of Nb

We have examined the problem of geometrical distortion from threefold symmetry in a single infinite chain, using a tight binding scheme (*5*) based on the extended Hückel method (*6*). The parameters of the calculation are described in the Appendix. The physical origin of the deformation is best revealed by calculations on "monomer" and "dimer" building blocks for the extended chain. These are defined as discrete mononuclear and binuclear complexes which retain the site symmetry and oxidation state of the transition metal centres in the infinite chain. Thus the "monomer" is $NbSe_6^{6-}$, **1**, and the "dimer" is $Nb_2Se_9^{6-}$, **2**. Each is examined in the undistorted equilateral triangle symmetry D_{3h} and in distorted C_{2v} geometries **3** and **4** based on an idealized structure of the actual extended solid.[1]

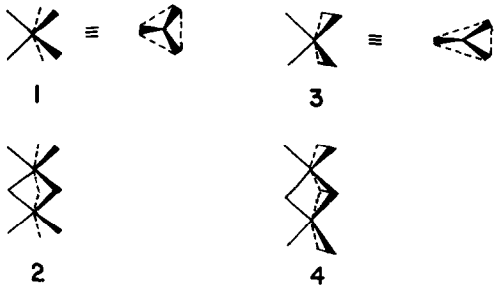

The energy levels of the monomer are shown at the left of Fig. 2. The *d*-block splitting is the expected $a_1'(z^2)$ and $e'(x^2-y^2, xy)$ below $e''(xz, yz)$ (*7*). The $a_1'-e'$ ordering and splitting is a function of the elongation or contraction of the trigonal prism. In the $NbSe_3$ geometry a_1' is at somewhat lower energy than e'. The figure shows only the highest orbital set, e'', derived from the six selenium atoms. Many other, primarily Se-based orbitals lie below.

The hole is clearly in the selenium orbitals, the Nb *d*-block lying empty. A schematic

[1] In the D_{3h} structure we took Se–Se 3.46, in the C_{2v} structure two Se–Se 3.79, one 2.40. Nb–Se was 2.65 in each case, Nb–Nb 3.48 Å.

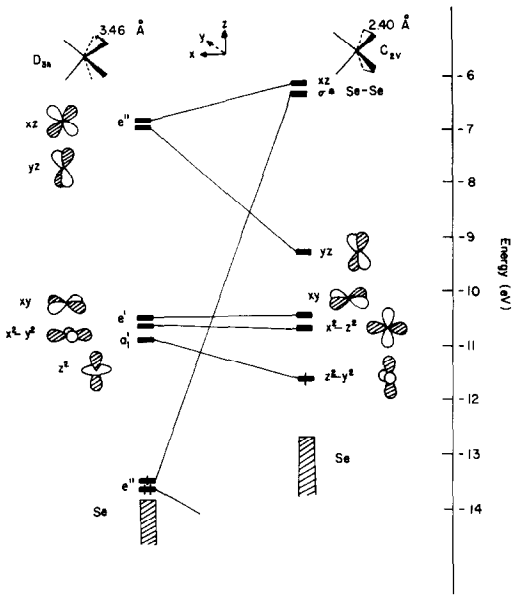

FIG. 2. The electronic structure of $NbSe_6^{6-}$ in D_{3h} and C_{2v} geometries.

drawing of one layer of the highest, partially occupied Se e'' level is shown in **5** and **6**. The view is along the threefold axis of the prism. The orbitals are best described as Se lone-pair combinations, reminiscent of the Walsh orbitals of cyclopropane.

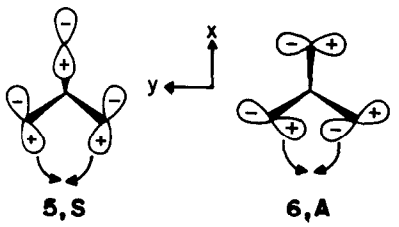

The distortion taking the D_{3h} structure into one resembling the correct geometry is indicated by arrows in **5** and **6**. Clearly **5**, symmetric with respect to the xz plane, will be stabilized, essentially forming a Se–Se σ bond. **6**, antisymmetric with respect to the xz plane, should be strongly destabilized in such a motion, and Fig. 2 shows clearly that it is. The antisymmetric level, Se–Se antibonding clearly rises above most of the Nb d-block. The unpaired electron finds a new home in the lowest Nb d-block orbital.

The above considerations, very simple in nature, help us to understand both the electronic structure and the deformation. The deformation is a kind of Jahn–Teller splitting, a breaking of the degeneracy of an $(e'')^3$ configuration. As a consequence of this distortion two Se ligands are transformed into a coordinated Se_2 ligand. In its complexed state it is best viewed as an analog of an η^2 dioxygen ligand, peroxidic in nature. Thus, if we must retain the oxidation state formalism, the actual situation is closer to $Nb^{4+}(Se^{2-})(Se_2^{2-})$, i.e., a d^1 Nb(IV), than it is to $Nb^{6+}(Se^{2-})_3$. These conclusions are not novel, having been stated in the literature earlier (*8*).

It should be noted that the breaking of the degeneracy of the $(e'')^3$ configuration is not of necessity stabilizing by itself. In our calculations on the monomer and dimer the distortion is in fact net destabilizing. If numcally reliable, this is an indirect sign that interchain interactions are required to produce a thermodynamically stable distortion.

Band Structures

A. Single $NbSe_3$ Chain

The effects of translational symmetry in one dimension along the **b**-axis are best approached through the band structure of

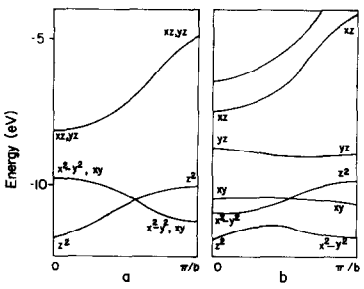

FIG. 3. The band structures of a single $NbSe_3$ chain for: (a) D_{3h} site symmetry and (b) C_{2v} site symmetry.

the hypothetical chain of D_{3h} site symmetry. This is shown in Fig. 3a. The d-block a_1', e', and e'' levels spread out into bands of substantial width, 1.5–3 eV. The interaction responsible for this is primarily a selenium coupling, since direct overlap of metal d-orbitals is small at this Nb–Nb separation. Here the d-block bands of Fig. 3a are empty as expected.

Note that the e' and a_1' bands interpenetrate. As the site symmetry is reduced to C_{2v} in the experimentally observed chain geometry the e' orbital degeneracy is lifted. The x^2-y^2 component of e' has the same reduced symmetry as the $z^2(a_1')$. The result is that both orbitals mix, and consequently, the resulting band structure (Fig. 3b) shows a typical avoided crossing, with variable z^2 and x^2-y^2 character at various points in the Brillouin zone. In this one-dimensional chain the lowest band is half-filled. The width of this band is very narrow (about 0.5 eV), so that the isolated $NbSe_3$ chain is more likely to be a magnetic insulator than a metal, like many facesharing octahedral MCl_3^- chains of transition metal ions (*5c, 9*).

The third band up is descended from the C_{2v} monomer xy orbital. The orientation of the monomer orbital, **7**, is important, for this orbital reaches out just in those directions

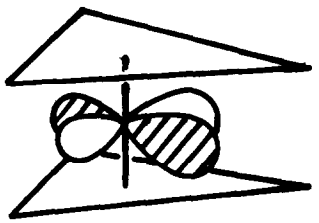

7

where Se atoms of neighbouring chains will be located. Thus it is anticipated that the flat xy band will be strongly perturbed as a two-dimensional structure along the c-axis is built in. Above these bands there are two metal xz and yz bands, and one derived primarily from Se–Se antibonding in a Se_2 bridging unit.

B. Interchain Interactions

Moving toward construction of the two-dimensional slab along the c-axis, let us first consider the band structure of a double chain **8** shown in Fig. 4b. The xy band of a single chain (Figs. 3b and 4a) near 10.5 eV is strongly perturbed and moves to the region of about 8 eV in a double chain (not shown in Fig. 4b), as outlined above. The other bands are generally doubled, the perturbation varying with the spatial extent of the metal d-orbitals. The d-block bands of Fig. 4b accomodate two electons and thus are partially filled. A limiting case of adding chains

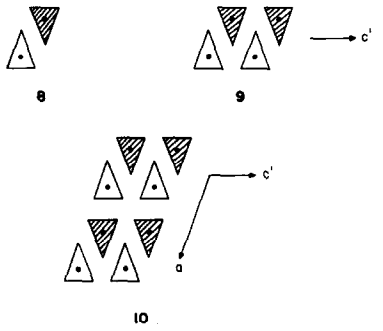

along the c-axis is the hypothetical two-dimensional slab **9** made by repeating a double chain along that axis. In **9**, $\mathbf{c}'$ is about $\mathbf{c}/3$. The band structure of **9** along the chain axis (b-axis) is shown in Fig. 4c. By comparing Figs. 4b and c, it is noted that the energy bands having the metal x^2-y^2 character are pushed above (not shown in Fig. 4c) as the two-dimensional structure is fully developed, leaving two overlapping bands of largely metal z^2 character and of substantial width (about 1.5–2.0 eV.).

That the x^2-y^2 character in the lower bands is diminished is not surprising. It is a reflection of the change in effective site symmetry upon interchain interaction. In the two-dimensional slab each Nb acquires two farther Se atoms in its coordination sphere, at distances only slightly longer than those within its own chain. The Nb environment

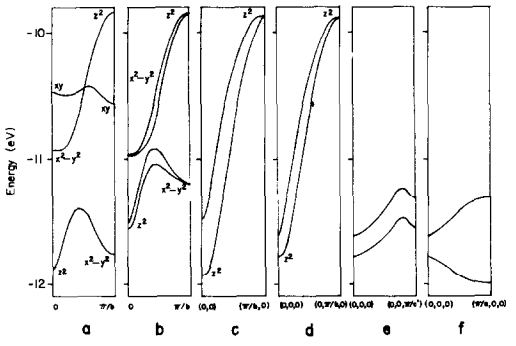

FIG. 4. The band structures of the model structures for: (a) a single $NbSe_3$ chain of C_{2v} site symmetry, (b) a double chain **8**, (c) the two-dimensional slab **9** along the chain axis (h_2, 0), (d) the three-dimensional structure **10** along the chain axis (0, k_2, 0), (e) that along the **c**'-axis (0, 0, k_3), and (f) that along the **a**-axis (k_1, 0, 0).

changes from six-coordinate, distorted trigonal prismatic, to an approximately eight-coordinate geometry. There are many closely related polytopes for eight-coordination, and this one could be described, not uniquely, as a distorted bicapped trigonal prism. The typical electronic feature of eight-coordination (*10*) is one orbital below four in the *d* block, the one separated here being described mainly as z^2.

To probe the interations between the two-dimensional slabs along the **a**-axis, we now consider the hypothetical unit cell **10** composed of a double chain, in which the unit-cell vectors **a** and **b** are the same as those of the real unit cell $(NbSe_3)_6$. Figures 4d, e, and f show respectively the band structures of **10** along the **b**-, **c**'-, and **a**-axes. The energy bands rise rapidly along the chain axis but vary slowly along the directions perpendicular to the chain axis, indicating a pseudo-one-dimensional nature for **10**. Further the energy bands of **10** along the chain direction are only slightly different from those of the two-dimensional slab **9**, which reveals that the ineractions between the two-dimensional slabs are weak.

The band structures of the real unit cell $(NbSe_3)_6$ along the **a**-, **b**-, and **c**-axes are respectively shown in Figs. 5a, b, and c. These bands now accommodate six electrons. In essence, these bands are similar to those of **10**. That is, $(NbSe_3)_6$ exhibits pseudo-one-dimensional character, as already noted by experiment (*1*) and theory (*2*). (To be more precise these lower bands, mainly z^2 in character, are of a one-dimensional nature. Higher energy bands based on xy and x^2-y^2 naturally show substantial dispersion in the plane perpendicular to the chain axes.) The bands of Fig. 5c (the bottom six) show less dispersion than those of Fig. 4e, due probably to the symmetry lowering along the **c**-axis in the real unit cell. The density of states calculated by Bullett shows that the Fermi level crosses only the bottom four bands of Fig. 5a, which results from the existence of the flat bands the directions perpendicular to the chain axis.

Discussion

The conduction bands in $NbSe_3$ are those shown in Fig. 5. The six bands which lie lowest at the Brillouin zone center are derived primarily from the niobium d_{z^2} orbitals, and are rather one dimensional throughout most of the Brillouin zone volume. At an energy of about −10 eV, two

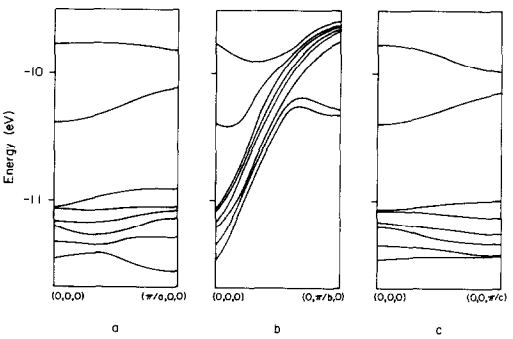

FIG. 5. The structures of the real $NbSe_3$ along (a) the **a**-axis (k_1, 0, 0), (b) the chain axis (0, k_2, 0), and (c) the **c**-axis (0, 0, k_3).

additional bands occur; these have predominatly $d_{x^2-y^2}$ character and are relatively dispersionless.

Although we have not performed an accurate density of states calculation, it is clear that the six electrons which must be accommodated into these eight bands will result in a Fermi level which lies at approximately −10.3 eV. The Fermi surface is therefore extremely complicated, consisting of sections from as many as seven bands. Due to the sensitivity of the exact positions and shapes of all these bands the atomic parameters used in the calculation, and to the positions of the atoms in the crystal, we hesitate to make explicit quantitative predictions. However several qualitative features are apparent.

The relatively dispersionless $d_{x^2-y^2}$ band(s) contributes the major part of the density of states at the Fermi surface. Their bandwidth of order 0.2 eV is consistent with the relatively large conduction electron magnetic susceptibility of order 10^{-4} cm^3/mole observed (*11*). Their contribution to the conductivity accounts for the small values observed (*12*) in the directions perpendicular to the **b**-axis, while the much larger conductivity along the **b**-axis (*1i*) is associated with the wider d_{z^2} bands, which have a highly one-dimensional character.

In view of the fact that our calculations indicate a very complicated Fermi surface topology, it is extremely difficult to deduce which sections contribute to the charge-density-wave (CDW) instabilities (*1g*). It is, however, quite clear that the two CDWs observed at low temperature are insufficient to create gaps at the Fermi surface for all the bands. Therefore the material remains metallic at low temperature and the sections of Fermi surface which survive can contribute to the recently observed (*1i*) superconductivity.

The exact details of the band structure and Fermi surface of niobium triselenide will continue to prove very difficult to deduce and to confirm. This arises in part because of the large number of atoms per unit cell of the crystal structure, and in part because the most sensitive experimental probes of the electronic structure are applied at low temperature where the charge-density-wave distortions have further lowered the symmetry of the lattice. The calculations which we have presented here reveal which atomic orbitals contribute to the bands near the Fermi surface, and thus give a good qualitative picture of the electronic structure of the material. This picture is in agreement with the relevant experimental results.

Appendix

The atomic parameters used in the present study are listed in the following table:

μ	ζ_μ	ζ'_μ	$H_{\mu\nu}$ (eV)
Se 4*s*	2.44[13]		−20.5[14]
Se 4*p*	2.07		−14.4
Nb 5*s*	1.90[15]		−10.1[16]
Nb 5*p*	1.85		−6.86
Nb 4*d*	4.08 (0.6401)	1.64 (0.5516)	−12.1

The *d* orbitals of Nb are given as a linear combination of two Slater-type functions and each is followed by the weighting coefficient in parentheses. A modified Wolfsberg–Helmholz formula (*17*) was used to calculate $H_{\mu\nu}$.

In all the band structure calculations, the lattice sums along the **a**-, **c**′-, and **c**-axes were taken up to the first-nearest neighbours. Along the **b**-axis, the lattice sum included up to the third-nearest neighbors in the case of the model structures but up to the first-nearest neighbors in the case of the real structure. In addition, the band structure calculations of the real unit cell did not

include the $5s$ and $5p$ atomic orbitals of Nb, so as to reduce the computational size. As confirmed by the band structures of **10** computed with the same procedure, the above basis set truncation does not affect the essential features of the band structures but shifts the d-block bands slightly upward.

Acknowledgments

The work at North Carolina State University was supported by the Petroleum Research Fund through Research Grant PRF11196-G6 and by the Faculty Research and Professional Development Fund through Grant TF-09223. M. -H. Whangbo wishes to thank Triangle Universities Computer Center for generous computer time. The work at Cornell was supported by NSF through Grant CHE7822048 and the Materials Science Center Grant DMR-7681083.

References

1. (*a*) P. MONCEAU, *Solid State Commun.* **24**, 331 (1977). (*b*) R. M. FLEMING, J. A. POLO, JR., AND R. V. COLEMAN, *Phys. Rev. B* **17**, 1634 (1978). (*c*) P. MONCEAU AND A. BRIGGS, *J. Phys. C* **11**, L465 (1978). (*d*) J. CHAUSSY, P. HAEN, J. C. LASJAUNIAS, P. MONCEAU, G. WAYSAND, A. WAINTAL, A. MEERSHAUT, P. MOLINIÉ, AND J. ROUXEL, *Solid State Commun.* **20**, 759 (1976). (*e*) P. MOLINIÉ, A. MEERSCHAUT, J. ROUXEL, P. MONCEAU, AND P. HAEN, *Nouv. J. Chim.* **1**, 205 (1977). (*f*) P. MONCEAU, M. P. ONG., A. M. PORTIS, A. MEERSCHAUT, AND P. MOLINIÉ, *Phys. Rev. Lett.* **37**, 602 (1976). (*g*) K. TSUTSUMI, T. TAKAGAKI, M. YAMAMOTO, Y. SHIOZAKI, M. IDO, T. SAMBONGI, K. YAMAYA, AND Y. ABE, *Phys. Rev. Lett.* **39**, 1675 (1977). (*h*) R. H. DEE, P. M. CHAIKIN, AND N. P. ONG, *Phys. Rev. Lett.* **42**, 1234 (1979). (*i*) C. M. BASTUSCHEK, R. A. BUHRMAN, J. D. KULICK, AND J. C. SCOTT, to be published.
2. D. W. BULLETT, *J. Phys. C* **12**, 277 (1979); *Solid State Commun.* **26**, 563 (1978).
3. J. L. HODEAU, M. MAREZIO, C. ROUCAU, R. AYROLES, A. MEERSCHAUT, J. ROUXEL, AND P. MONCEAU, *J. Phys. C* **11**, 4117 (1978).
4. (*a*) O. FOSS AND V. JANICKIS, *J. Chem. Soc. Chem. Commun.*, 834 (1977); P. CHERIN AND P. UNGER, *Acta Crystallogr. Sect. B* **28**, 313 (1972). (*b*) C. M. WOODWARD, D. S. BROWN, J. D. LEE, AND A. G. MASSEY, *J. Organometal. Chem.* **121**, 33 (1976); C. J. MARSDEN AND G. M. SHELDRICK, *J. Mol. Struct.* **10**, 419 (1971). (*c*) M. G. B. DREW, G. W. A. FOWLES, E. M. PAGE, AND D. A. RICE, *J. Amer. Chem. Soc.* **101**, 5827 (1979).
5. (*a*) M.-H. WHANGBO AND R. HOFFMANN, *J. Amer. Chem. Soc.* **100**, 6093 (1978). (*b*) M.-H. WHANGBO, R. HOFFMANN, AND R. B. WOODWARD, *Proc. Roy. Soc. Ser. A* **366**, 23 (1979). (*c*) M. -H. WHANGBO, M. J. FOSHEE, AND R. HOFFMANN, *Inorg. Chem.* (1979), in press.
6. R. HOFFMANN, *J. Chem. Phys.* **39**, 1397 (1963); R. HOFFMANN AND W. N. LIPSCOMB, *J. Chem. Phys.* **36**, 2179, 3489 (1962); **37**, 2872 (1962).
7. (*a*) E. I. STIEFEL, R. EISENBERG, R. C. ROSENBERG, AND H. B. GRAY, *J. Amer. Chem. Soc.* **88**, 2956 (1966). (*b*) G. N. SCHRAUZER AND V. P. MAYWEG, *J. Amer. Chem. Soc.* **88**, 3234 (1966). (*c*) F. HULLIGER, *Struct. Bonding (Berlin)* **4**, 83 (1968). (*d*) K. ANZENHOFER, J. M. VAN DEN BERG, P. COSSEE, AND J. N. HELLE, *J. Phys. Chem. Solids* **31**, 1057 (1970). (*e*) A. A. G. TOMLINSON, *J. Chem. Soc. A*, 1409 (1971). (*f*) W. O. GILLUM, R. A. D. WENTWORTH, AND R. F. CHILDERS, *Inorg. Chem.* **9**, 1825 (1970); R. A. D. WENTWORTH, *Coord. Chem. Rev.* **9**, 171 (1972). (*g*) R. HUISMAN, R. DEJONGE, C. HAAS, AND F. JELLINEK, *J. Solid State Chem.* **3**, 56 (1971). (*h*) E. LARSEN, G. N. LAMAR, B. F. WAGNER, J. E. PARKS, AND R. H. HOLM, *Inorg. Chem.* **11**, 2652 (1972). (*i*) R. HOFFMANN, J. M. HOWELL, AND A. R. ROSSI, *J. Amer. Chem. Soc.* **98**, 2484 (1976).
8. (*a*) F. JELLINEK, R. A. POLLAK, AND M. W. SHAFER, *Mater. Res. Bull.* **9**, 845 (1974). (*b*) J. A. WILSON: *Phys. Rev. B* **19**, 6546 (1979).
9. (*a*) B. H. BRANDOW, *Advan. Phys.* **26**, 651 (1977), and references therein; *J. Quantum Chem. Symp.* **10**, 417 (1976). (*b*) M.-H. WHANGBO, *J. Chem. Phys.* **70**, 4963 (1979); *Inorg. Chem.* (1979), in press.
10. J. K. BURDETT, R. HOFFMANN, AND R. C. FAY, *Inorg. Chem.* **17**, 2553 (1978).
11. J. D., KULICK AND J. C. SCOTT, *Solid State Commun.*, in press.
12. P. MONCEAU, J. PEYRARD, J. RICHARD, AND P. MOLINIÉ *Phys. Rev. Lett.* **39**, 160 (1977); N. P. ONG AND J. W. BRILL, *Phys. Rev. B* **18**, 5265 (1978).
13. E. CLEMENTI AND C. ROETTI, *At. Data Nucl. Data Tables* **14**, 177 (1974).
14. J. HINZE AND H. H. JAFFÉ, *J. Phys. Chem.* **67**, 1501 (1963).
15. H. BASCH AND H. B. GRAY, *Theor. Chim. Acta* **4**, 367 (1966).
16. R. H. SUMMERVILLE AND R. HOFFMANN, *J. Amer. Chem. Soc.* **98**, 7240 (1976).
17. J. H. AMMETER, H.-B. BÜRGI, J. C. THIBEAULT, AND R. HOFFMANN, *J. Amer. Chem. Soc.* **100**, 3686 (1978).